

Recent advances in compact repetitive high-power Marx generators

Falun Song¹, Fei Li¹, Beizhen Zhang¹, Mingdong Zhu^{1,2}, Chunxia Li¹, Ganping Wang¹, Haitao Gong¹, Yanqing Gan¹ and Xiao Jin¹

Research Article

Cite this article: Song F, Li F, Zhang B, Zhu M, Li C, Wang G, Gong H, Gan Y, Jin X (2019). Recent advances in compact repetitive high-power Marx generators. *Laser and Particle Beams* **37**, 110–121. <https://doi.org/10.1017/S0263034619000272>

Received: 24 January 2019
Revised: 5 March 2019
Accepted: 5 March 2019

Key words:

High power; Marx generator; pulse-forming module; pulsed power; repetitive

Author for correspondence:

Falun Song, Science and Technology on High Power Microwave Laboratory, Institute of Applied Electronics, China Academy of Engineering Physics, Mianyang 621900, China. E-mail: songfalun@caep.cn

¹Science and Technology on High Power Microwave Laboratory, Institute of Applied Electronics, China Academy of Engineering Physics, Mianyang 621900, China and ²China State Key Laboratory of Advanced Welding and Joining, Harbin Institute of Technology, Harbin 150001, China

Abstract

This paper introduces recent activities on Marx-based compact repetitive pulsed power generators at the Institute of Applied Electronics (IAE), China Academy of Engineering Physics (CAEP), over the period 2010–2018. A characteristic feature of the generators described is the use of a simplified bipolar charged Marx circuit, in which the normal isolation resistors or inductors to ground are removed to make the circuit simpler. Several pulse-forming modules developed to generate a 100 ns square wave output are introduced, including thin-film dielectric lines of different structures, a pulse-forming line based on a Printed Circuit Board, and non-uniform pulse-forming networks. A compact repetitive three-electrode spark gap switch with low-jitter, high-voltage, and high-current was developed and is used in the generators. A positive and negative series resonant constant current power supply with high precision and high power is introduced. As an important part of the repetitive pulse power generator, a lower jitter pulse trigger source is introduced. Several typical high-power repetitive pulsed power generators developed at IAE are introduced including a 30 GW low-impedance Marx generator, a compact square-wave pulse generator based on Kapton-film dielectric Blumlein line, a 20 GW high pulse-energy repetitive PFN-Marx generator, and a coaxial Marx generator based on ceramic capacitors. The research of key technologies and their development status are discussed, which can provide a reference for the future development and application of miniaturization of compact and repetitive Marx generators.

Introduction

Since the 1990s, pulsed power technology has continued to progress in the direction of ultra-high power and high-energy of single-pulse systems to meet the needs of flash radiography, X-ray generation, inertial confinement fusion, and so on (Quintenz, 2004; Deng *et al.*, 2015, 2016; Ding *et al.*, 2016). At the same time, driven by the demand for directed energy applications such as high-power microwaves, the development of compact repetitive pulsed power technology is accelerating (Gaudet *et al.*, 2004; Kim *et al.*, 2016). Initially, miniaturization of high-power microwave systems was focused on high-power microwave devices. As the mobility requirements of high-power microwave systems have increased, research has begun to pay more and more attention to the miniaturization of pulsed power sources (Korovin *et al.*, 2004; Pan *et al.*, 2016; Zhang *et al.*, 2016). The Multidisciplinary University Research Initiative (MURI) program on compact, portable, pulsed power that began in the USA in 2001 (Gaudet *et al.*, 2004) was mainly focused on the fundamental research on the essential components of compact pulsed power for directed energy application. A series of compact pulsed power generators based on Tesla transformers and their applications has been developed and researched in Russia (Mesyats *et al.*, 2003, 2004; Kim *et al.*, 2016). Compact repetitive pulsed power research began at IAE in the early 2000s with the development of helical high-current accelerator (650 kV, 6.5 kA, 210 ns, 20 Hz) (Cao *et al.*, 2006). IAE developed a further type of pulse accelerator (1 MV, 20 kA, 40 ns, 100 Hz) based on Tesla transformer in 2006 (Zhang *et al.*, 2007), followed by a repetitive pulse generator (800 kV, 8.5 GW, 180 ns, 25 Hz) based on a Linear Transformer Driver (LTD) in 2010 (Xiang *et al.*, 2010). Though the three pulsed power systems mentioned above have a good performance and repeatability, their sizes and weights are still too large. Since 2010, IAE has embarked on more compact pulsed power system research. In order to minimize the size and weight, a simplified bipolar charged Marx circuit was proposed with a series of pulsed power generators developed based on the simplified Marx circuit. The detailed simplification of the Marx circuit is described in section “Simplification of Marx circuit”. Research and developments on several key technologies and components, such as compact pulse-forming modules, a compact and

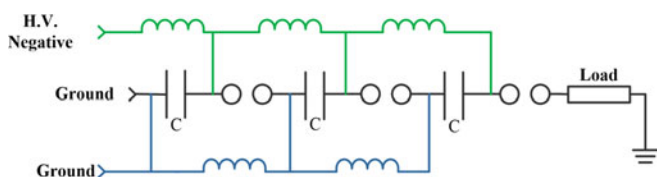


Fig. 1. A typical single-sided charged Marx generator.

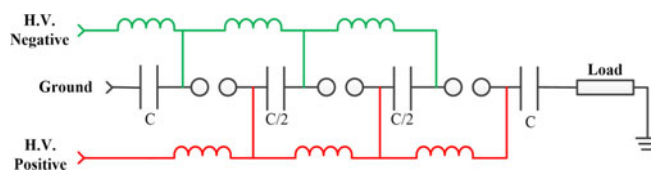


Fig. 3. Simplified bipolar charged Marx generator.

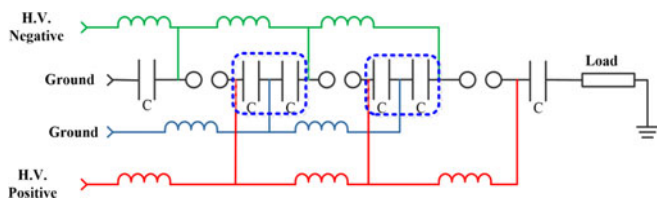


Fig. 2. A typical bipolar charged Marx generator.

repetitively triggered spark-gap switch, a high-voltage bipolar charging power supply with high precision and high average power, and a fast rise-time trigger source with low jitter and high energy are presented in section “Continuing research and development of key technologies and vital components”. Several typical compact repetitive Marx generators are described in section “Development of repetitive pulsed power generators”.

Simplification of Marx circuit

The Marx circuit widely used in the high-power pulsed generators is a voltage-multiplying circuit that charges a number of capacitors in parallel and discharges them in series (Lehr and Ron, 2017). Figure 1 shows a typical single-sided charged Marx generator, where a number N of switches and of capacitors are used, producing an open-circuit voltage of NV_0 (where V_0 is the charging voltage). A bipolar charged Marx circuit is shown in Figure 2, where N switches and $2N$ capacitors are used, producing an open-circuit voltage of $2NV_0$. The advantage of this bipolar charged Marx circuit is that it has half the number of switches but twice the stage voltage for a given output voltage. An isolation resistor to ground is connected between the two capacitors of each stage in the conventional bipolar charged Marx generator, as shown in Figure 2. The isolation resistor chain may be replaced by an inductor chain to enable faster charging and to attain the capability of repetitive operation, and reduce the time of electric stress on the insulation during charging.

Without affecting the basic characteristics of the Marx circuit, removal of the grounding resistors from the Marx circuit and the combination of two capacitors of the same stage into one capacitor will further simplify the circuit, as shown in Figure 3. The capacitance of the first and last capacitors are both C_0 , and the capacitance of 2^{nd} to $(N-1)^{th}$ are $C_0/2$. If the capacitors are replaced by pulse-forming lines (PFL) or pulse-forming networks (PFN), an output pulse with flat-top duration can be obtained, as shown in Figure 4, where the waveform obtained using the simplified Marx circuit is the same as that of the conventional bipolar charged Marx circuit. This simplified Marx circuit reduces the number of capacitors and eliminates the resistors to ground, which facilitates miniaturization of the pulsed power system.

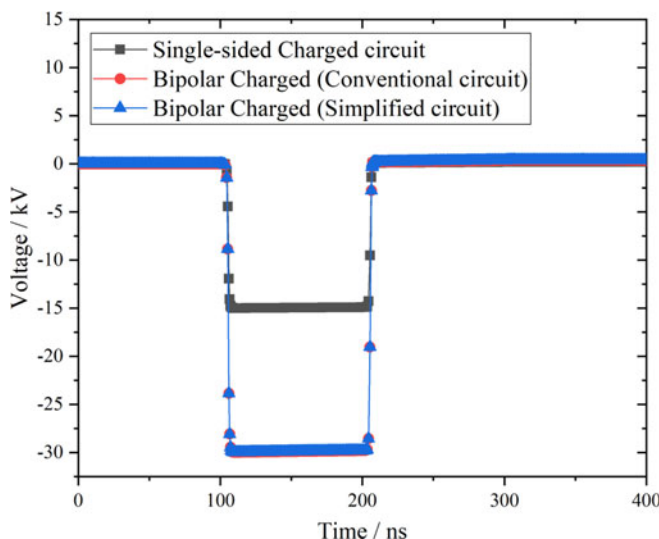


Fig. 4. Comparison of the output waveforms using three types of Marx circuits based on PFL.

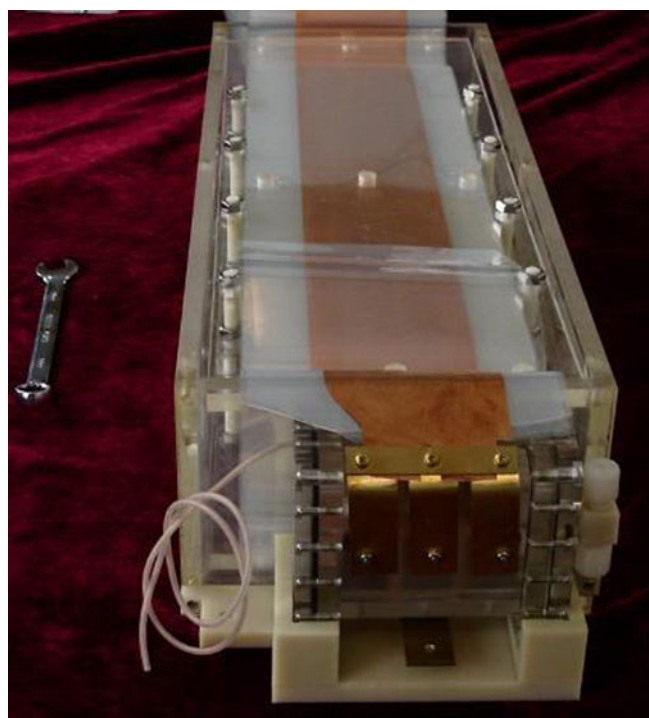


Fig. 5. Compact, portable layer-wound Blumlein line.

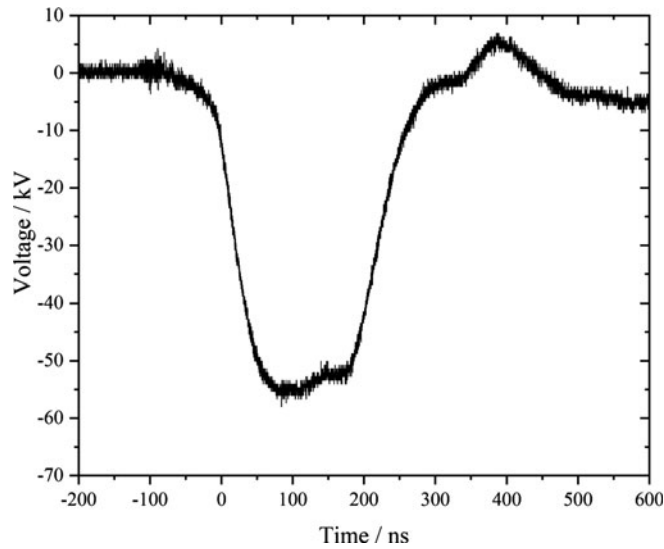


Fig. 6. Output waveform of layer-wound Blumlein line.

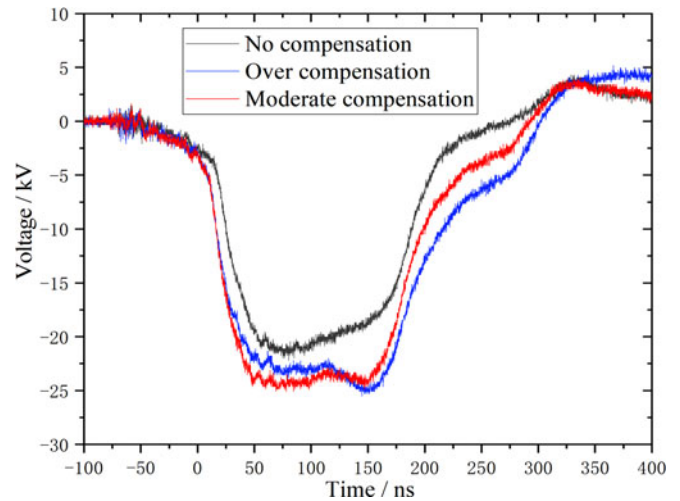


Fig. 8. Output waveforms of the thin plate-isolated Blumlein line with and without impedance compensation.



Fig. 7. The thin plate-isolated Blumlein lines.

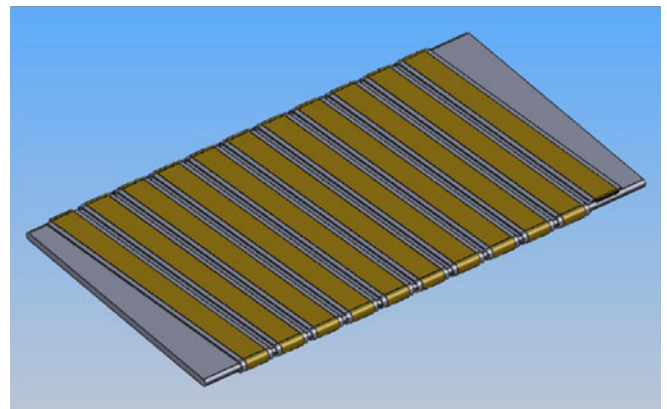


Fig. 9. Schematic of a layer-wound spiral strip line.

Continuing research and development of key technologies and vital components

Pulse-forming modules

Several different kinds of pulsed forming modules were developed at IAE, such as thin-film dielectric PFLs, PFL based on Printed Circuit Board (PCB), and non-uniform PFN. Thin-film dielectric PFL is easy to fold and wind (Smith *et al.*, 1971; Schamiloglu *et al.*, 2003; Ouyang *et al.*, 2008), which is beneficial to the miniaturization of pulse power sources. Figure 5 shows a compact, portable, layer-wound mylar dielectric Blumlein line, having the dimensions of 50 cm × 18 cm × 12 cm, maximum withstand voltage of 60 kV, and a pulse width of 180 ns (Gan *et al.*, 2012). Figure 6 shows the typical output waveform of a

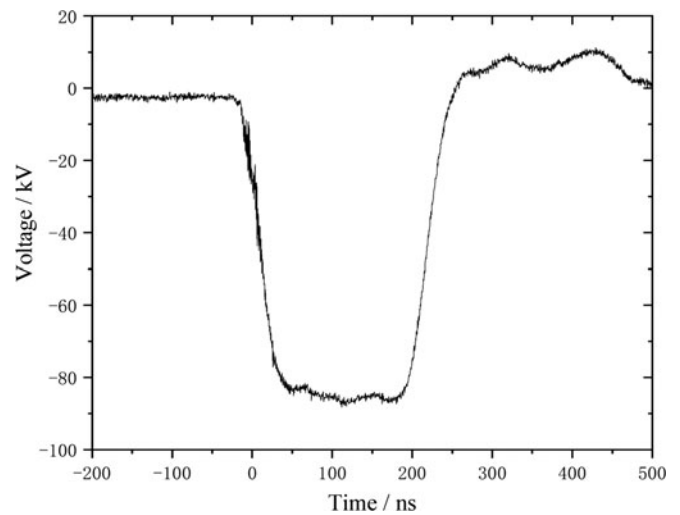


Fig. 10. Output waveform of spiral strip line with charging voltage of 100 kV.

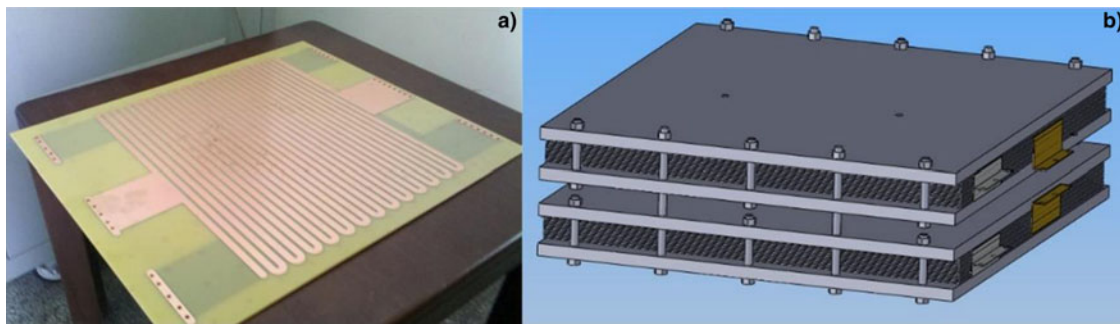


Fig. 11. S-type folded planar pulse-forming line based on PCB, (a) single module, (b) multi-stage parallel modules.

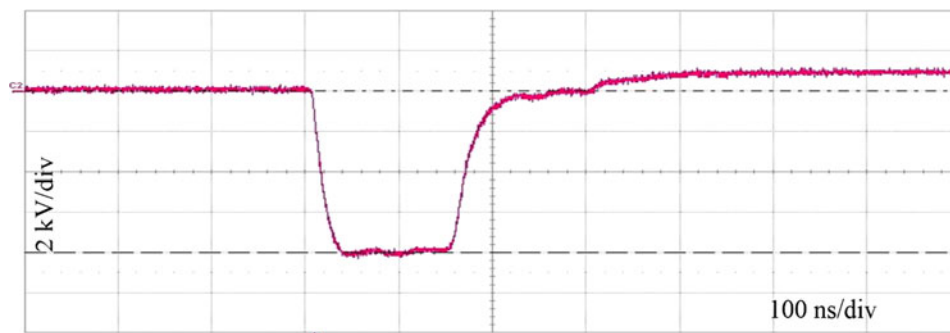


Fig. 12. Output waveform of S-type folded planar PFL.

layer-wound Blumlein line. As can be seen that there is a pre-pulse about 90 ns before the voltage waveform due to the spatial electric field coupling to the load. Affected by the coupling effect, the pulse amplitude decreases during the second half of the main pulse.

In order to reduce the influence of the coupling effect on the flat-top of the pulse waveform, the characteristic impedance of the second half of the Blumlein line is changed to a gradient impedance to compensate the output waveform. Figure 7 shows the thin plate-isolated Blumlein lines. The output waveforms before and after impedance compensation were shown in Figure 8. The results show that a waveform with a better flat-top is obtained after the compensation.

A spiral strip Blumlein line with a withstand voltage of 100 kV and a pulse width of ~200 ns was developed (Song *et al.*, 2012). This type of line is spirally wound on a flat insulator of Polymethyl methacrylate, as shown in Figure 9. This type of PFL has a relatively wide pitch and layer spacing, so the output waveform is not affected by the coupling effect, and the spiral winding makes the structure more compact. The thickness of the thin-film dielectric layer is determined by the designed characteristic impedance and withstand voltage. An output waveform with a rise time of 40 ns, a pulse width of 207 ns, and a flat-top of 140 ns is obtained, as is clear from Figure 10.

In order to meet the requirement of a relatively low-power pulsed system, a more compact solid-state PFL based on a PCB was developed (Li *et al.*, 2013). Figure 11a shows a planar S-type folded PFL with a withstand voltage of 50 kV. A multi-stage PFL module was designed in parallel in order to reduce

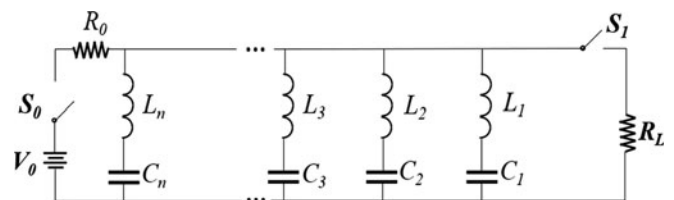


Fig. 13. Equivalent circuit for Guillemin type C network with n branches.

the characteristic impedance and improve the energy-storage density, as shown in Figure 11b. A typical output waveform having a pulse width of 140 ns and a flat-top width of 100 ns is shown in Figure 12. This kind of PFL has a pulse square wave with good flat-top, but a low withstand voltage due to the limitation of the dielectric material of PCB. It is suitable for use in relatively low-power, low-voltage pulsed circuits.

The PFN is a typical square wave pulse-forming technique using L-C circuit. Figure 13 shows an equivalent electrical circuit for the Guillemin type C network with n branches (Li *et al.*, 2018). The experimental results show that when the L-C cell number of the Guillemin type C network is gradually reduced from 6 to 2, a good square-wave pulse can still be obtained, as shown in Figure 14. Therefore, in attempts to obtain a quasi-square waveform with flat-top under a compact structure, a low-inductance pulse-forming module based on two-cell L-C circuit was designed and fabricated (Li *et al.*, 2018). The two-cell PFN was encapsulated in a shell and

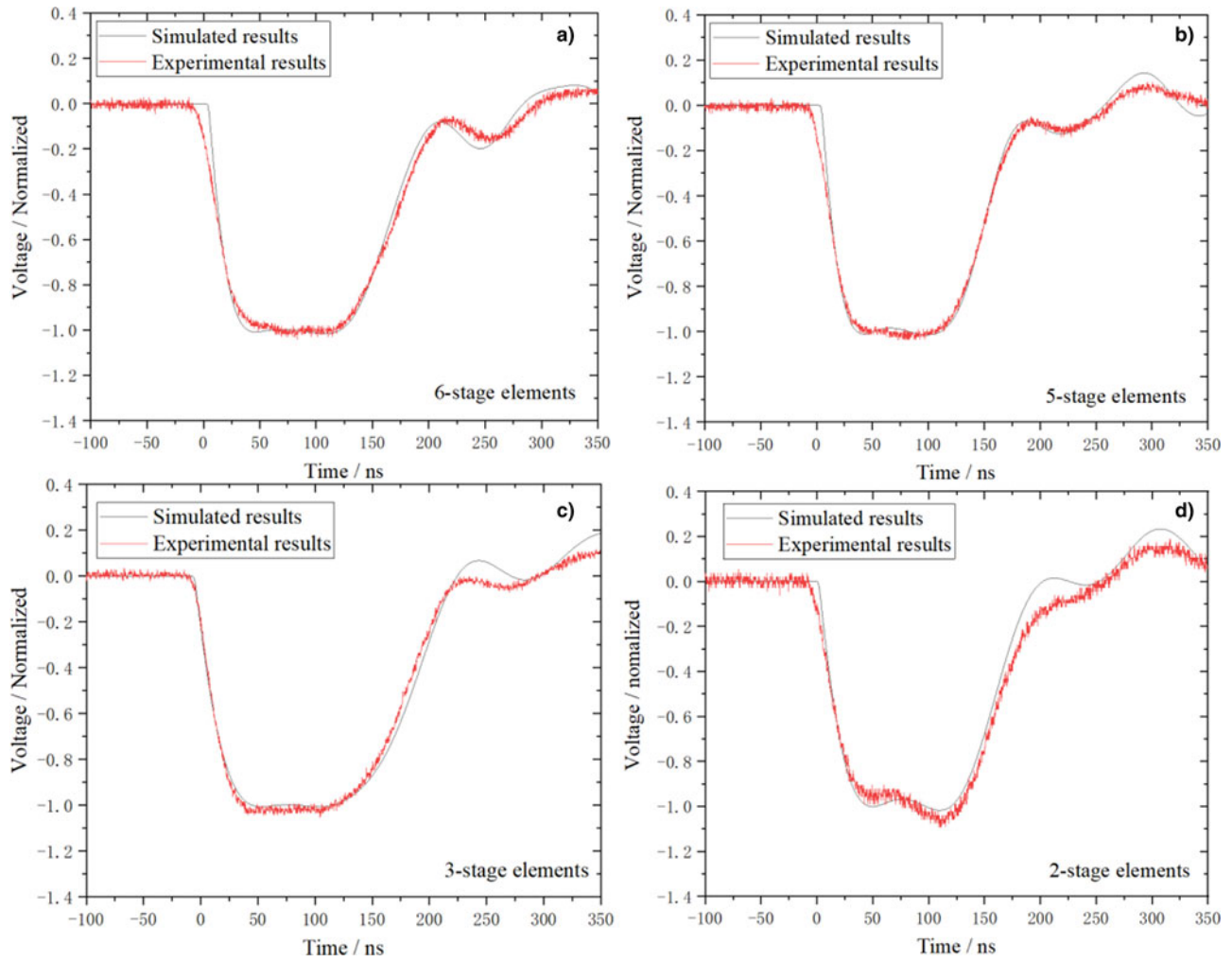


Fig. 14. Experimental and simulated results of different branches of Guillemin network.

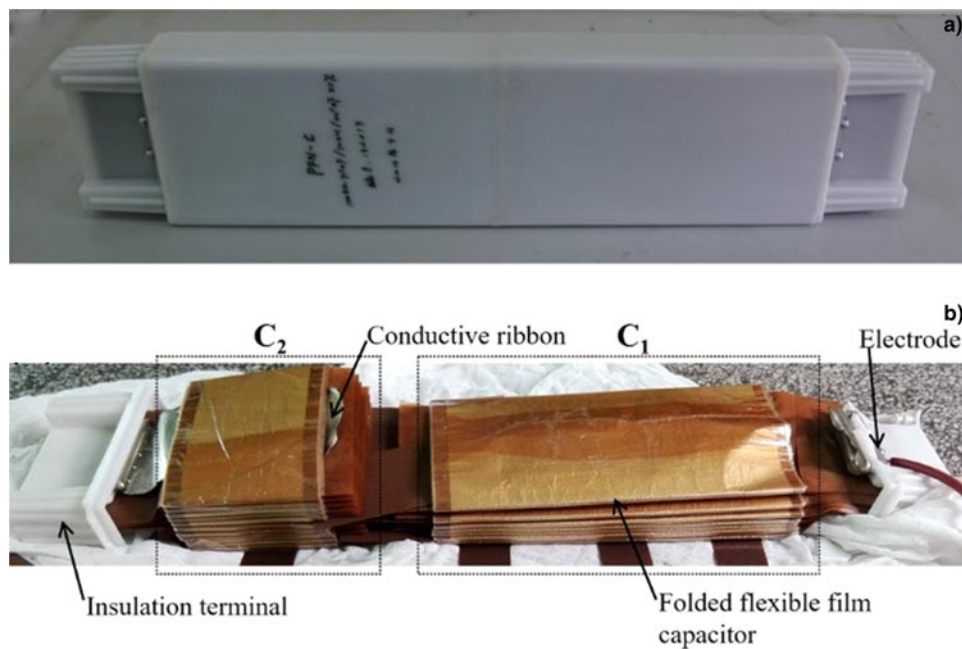


Fig. 15. Picture of the pulse-forming module and internal structures.

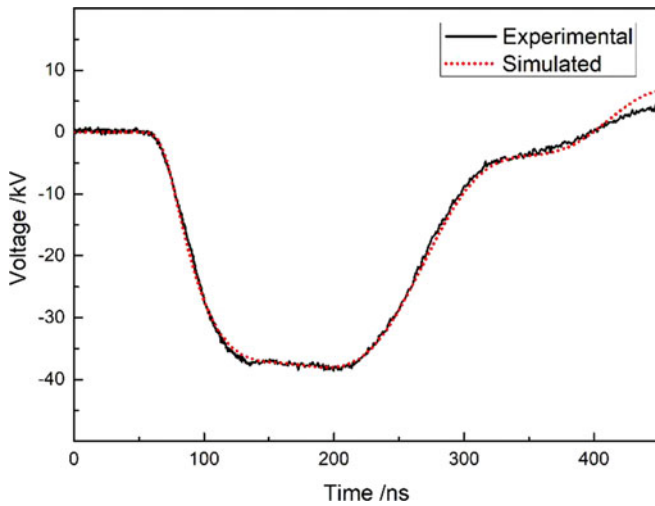


Fig. 16. Simulated and experimental output waveforms.

appears similar to a conventional capacitor, as shown in Figure 15. The dimensions of the two-cell pulse-forming module with an impedance of 2.5Ω are $720 \text{ mm} \times 155 \text{ mm} \times 62 \text{ mm}$, and its energy storage density can reach 42 kJ m^{-3} . The research results show that the developed pulse-forming module has a withstand voltage of 120 kV, a pulse of 180 ns, and a flat-top of 100 ns. Simulated and experimental output waveforms are given in Figure 16.

Three-electrode spark-gap switch with low jitter and high current

The spark-gap switch is a key component of an only pulsed power source with the performance of the switch directly influencing the output characteristics of the overall pulsed power system. Based on the application requirements of the repetitive pulsed power source, a small field distortion three-electrode spark gap switch was designed, developed, and studied (Zhang *et al.*, 2018), as shown in Figure 17. The compact switch has a small size of only $150 \text{ mm} \times 42 \text{ mm}$, a light weight of about 1.5 kg, and a high withstand voltage of over 112 kV. The switch filled with a mixed gas of 30% SF_6 and 70% N_2 has a wide voltage operating range of 31–90, 42–85% of the pulsed self-breakdown voltage at the gas pressures of 0.1, 0.4 MPa, as shown in Figure 18. It can be operated stably at a repetition rate between 1 and 50 Hz with a jitter of $<4 \text{ ns}$, as shown in Figure 19. Its service life has exceeded 100 000 shots under the on-current of 8.5 kA.

High precision and high-power repetitive power supply

Since there are no resistors or inductors to ground in a simplified Marx circuit, the potential of the capacitors is suspended during charging, which causes the positive and negative voltages of a capacitor to be inconsistent or even impossible to be charged. A special constant current charging power system was therefore developed (Gan *et al.*, 2018), as shown in Figure 20. A real-time comparison circuit was used in the control mode. After each small step is completed, the control system compares the positive and negative voltages so as to confirm whether they

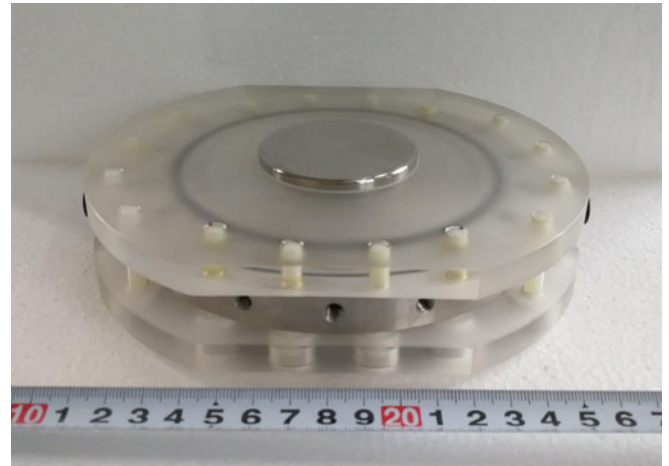


Fig. 17. Photo of the small field distortion spark-gap switch.

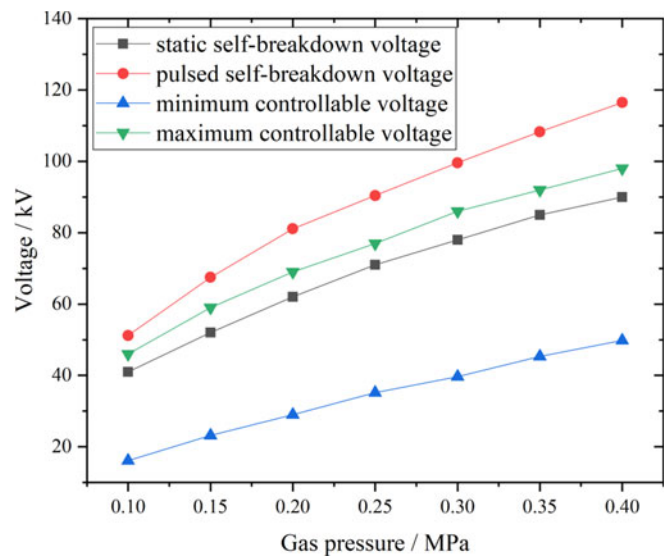


Fig. 18. Operating voltage range of the switch versus gas pressure.

are consistent. If there is a deviation, the part with larger voltage is hold constant with the other part adjusted until the two voltages are equal. Then the joint charges are continued and repeated iteratively in order to realize the positive and negative voltage synchronous charging. Figure 21 gives the real-time comparison charging schematic.

Based on this design idea, a compact high-power pulse charging power supply was developed, with an output voltage between ± 10 and $\pm 50 \text{ kV}$, a charging accuracy of 0.1 kV, a charging current of 2.5 A, and a repetition frequency continuously adjustable between 1 and 50 Hz. The power supply has a small volume of $1.7 \text{ m} \times 1.5 \text{ m} \times 0.5 \text{ m}$, a light weight of 300 kg, with strong anti-interference abilities and a short-circuit capability. In practice, it has been applied to a repetitively high-power pulse power source.

Low-jitter high-energy trigger source

In order to reduce the delay time jitter of a repetitive pulse generator, a low-jitter and repetitively high-energy trigger source was

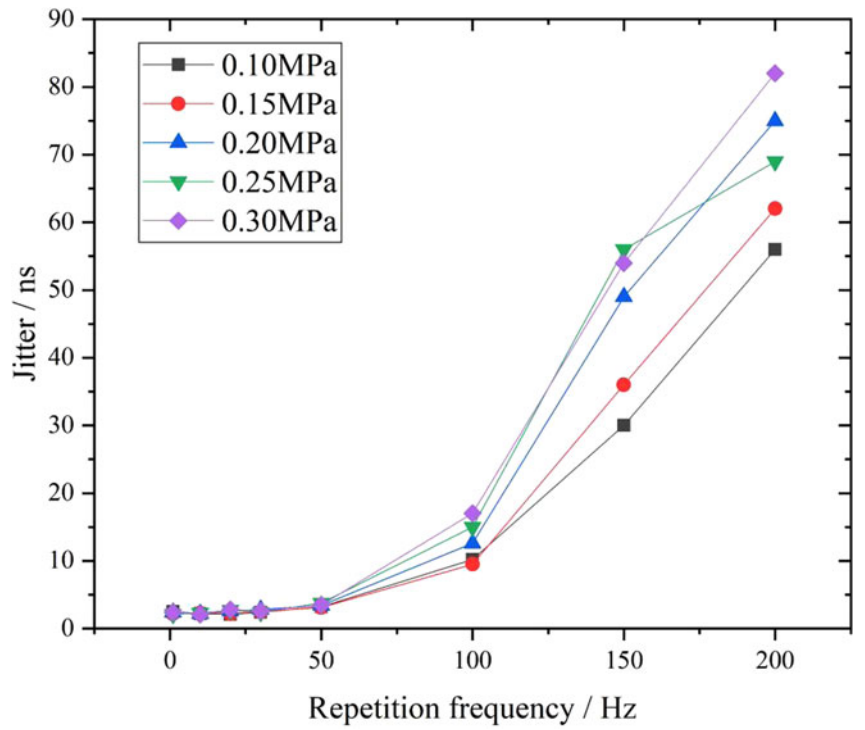


Fig. 19. Variation of jitter with the repetition frequency.

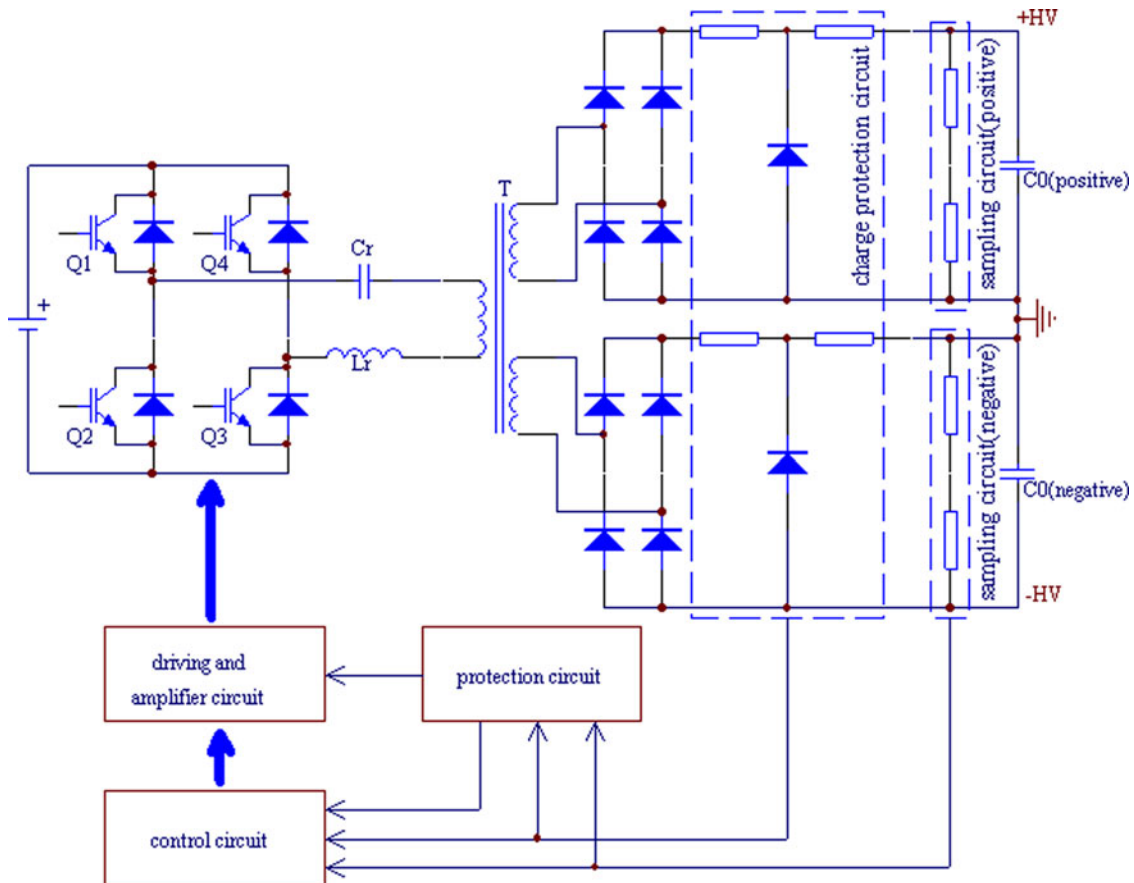


Fig. 20. Equivalent circuit of series resonant charger.

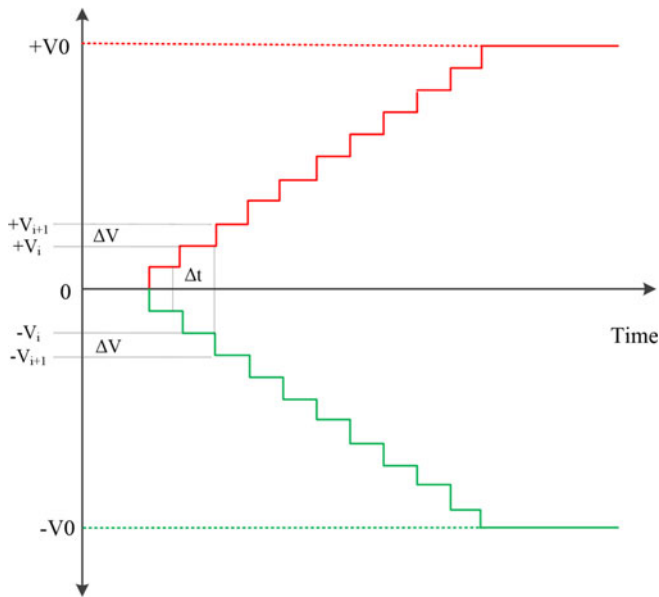


Fig. 21. A step comparison charging schematic.

developed (Li *et al.*, 2017). The source consists of a ± 50 kV charging power supply, a Hydrogen-thyristor pulse source with an output voltage of 80 kV, two 30 nF capacitors, a three-electrode spark gap switch, and a high-power solid resistor of 300 Ω , as shown in Figure 22. The output pulse has a rise time of 30 ns, a width of 200 ns, a maximum output voltage of 95 kV, and a maximum storage energy of 75 J. It can run with 30 pulses at a repetition rate of 30 Hz and a jitter of only 2 ns, as shown in Figure 23.

Development of repetitive pulsed power generators

Low-impedance Marx generator

A low-impedance Marx generator with an output voltage of 628 kV, a current of 52 kA, a rise time of 97 ns, a storage energy

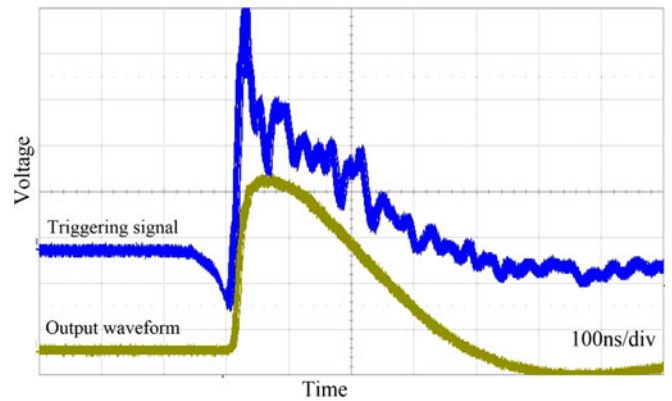


Fig. 23. Output waveforms of high-energy trigger source.

of 5 kJ, and dimensions of 1.2 m \times 0.5 m \times 0.6 m was developed (Qin *et al.*, 2012), as shown in Figure 24. Based on this generator, a low-impedance magnetically insulated line oscillator (MILO) was directly driven (Song *et al.*, 2013). With an electron-beam voltage of ~ 450 kV and a current of ~ 40 kA, the radiated microwave had a peak power of 400 MW, a pulse width of 60 ns, and the center frequency of 1.23 GHz. Figure 25 shows the voltage and current waveforms of the low-impedance Marx generator with a MILO as the load.

Square-wave pulse generator based on Kapton-film dielectric line

A square-wave pulse generator based on Kapton-film dielectric Blumlein line using the simplified Marx circuit was developed (Song *et al.*, 2017b), as shown in Figure 26. The output pulse obtained had a peak power of 4 GW, a width of 156 ns, a rise time of 40 ns when feeding on a 60 Ω water resistor load. It could be operated at a repetition rate of 10 Hz. Figure 27 shows the output waveform in both single shot and a repetition rate of 10 Hz.

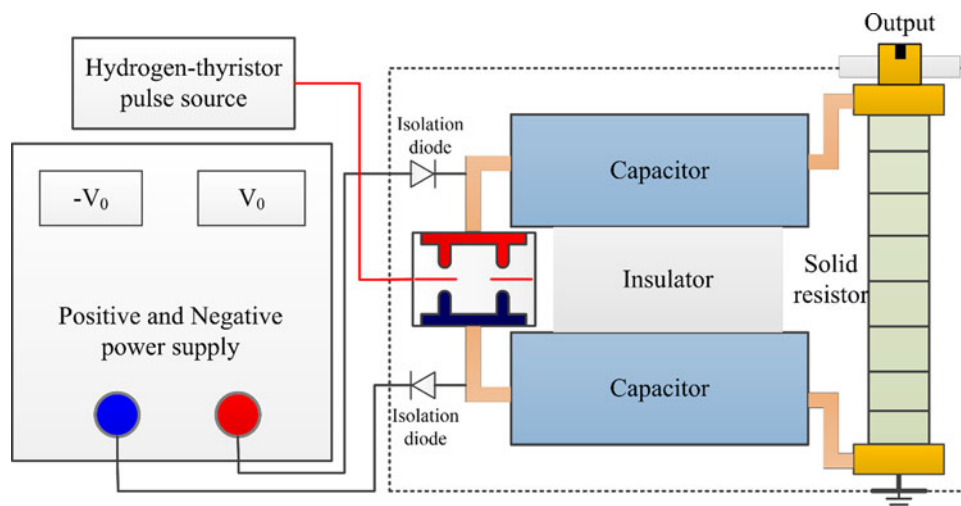


Fig. 22. Layout of the high-energy trigger source.

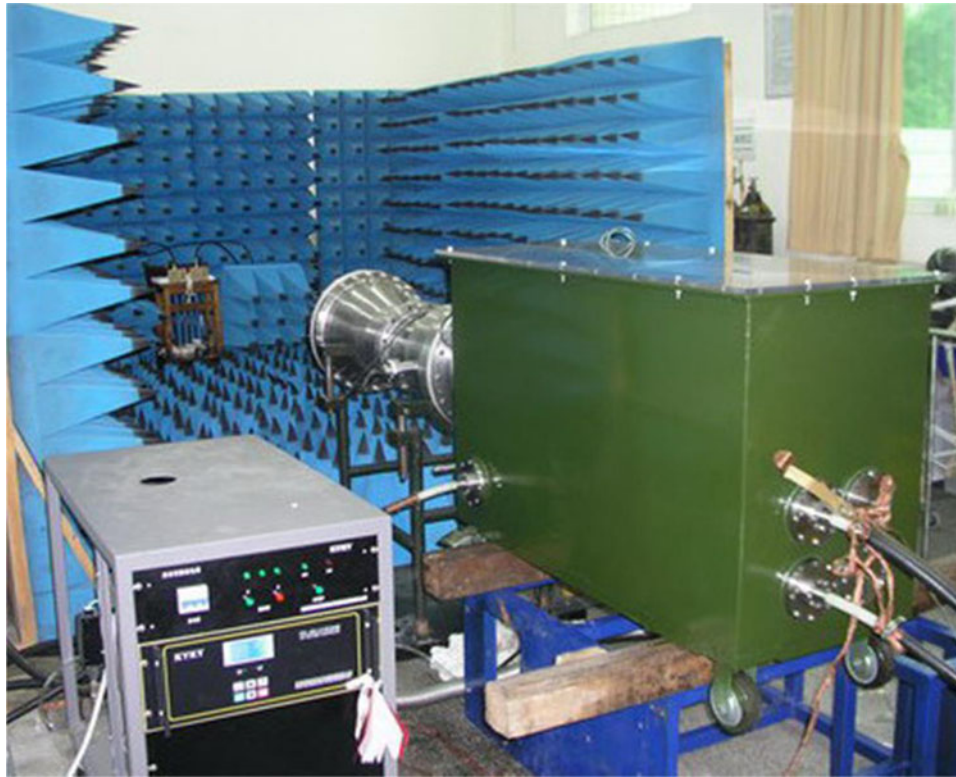


Fig. 24. Photo of a low-impedance Marx generator for high-power microwave application.

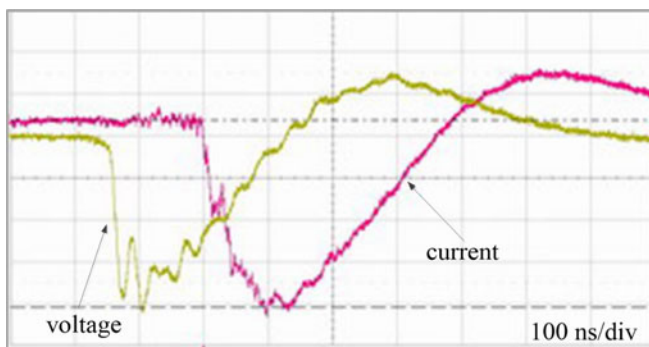


Fig. 25. Voltage and current waveforms of low-impedance Marx generator.

High pulse-energy repetitive PFN-Marx generator

A compact and repetitively high pulse-energy PFN-Marx generator with low jitter was developed using the simplified bipolar Marx circuit (Song *et al.*, 2017a, 2019), as shown in Figure 28. The size and weight of the generator were minimized by using two-cell pulse-forming modules as described earlier, alternating two superposition structures on both sides and high electric field shielding technology. The generator has a total volume of 2.5 m³ and a weight of 2.2 tons, making it much more compact than conventional pulsed power sources. Experimental results demonstrated that when the generator operates with a single pulse output, the voltage, current, and peak power are 0.98 MV, 19.6 kA, and 19.2 GW. The total energy storage in the Marx

tank is about 3.9 kJ. When the generator was operated at a repetition rate of 30 Hz, the output pulse had a peak power of 16.7 GW obtained as shown in Figure 29. The voltage fluctuation range is limited to within $\pm 1.5\%$, and the current fluctuation range is limited to within $\pm 2\%$. The delay time jitter between the trigger pulse and the output pulse is < 6.5 ns standard mean deviation. Statistical distributions of the delay time jitter and current amplitude variation of the 300 pulses are approximately Gaussian.

Coaxial Marx generator based on ceramic capacitors

A compact coaxial Marx generator with a 3.3 nF ceramic capacitor as the stage storage capacitance was developed (Gan *et al.*, 2013). When operating at a repetition rate of 100 Hz, a pulse with a voltage of 150 kV, a width of 25 ns, and a rise time of 10 ns was obtained on a 50 Ω resistive load. The maximum voltage can reach 240 kV on open circuit. Figure 30 shows the generator, which is $\Phi 200$ mm \times 550 mm in size, and Figure 31 shows a typical output waveform with an output voltage of 100 kV.

Conclusion

This paper reviews the progress of the miniaturization of repetitive pulsed power sources in recent years at IAE. A simplified bipolar Marx circuit was proposed and has been applied to the development of various types of compact pulsed power sources, laying a foundation for future miniaturization and practical application. The development of pulsed power



Fig. 26. Photo of pulse generator based on Kapton-film dielectric line.

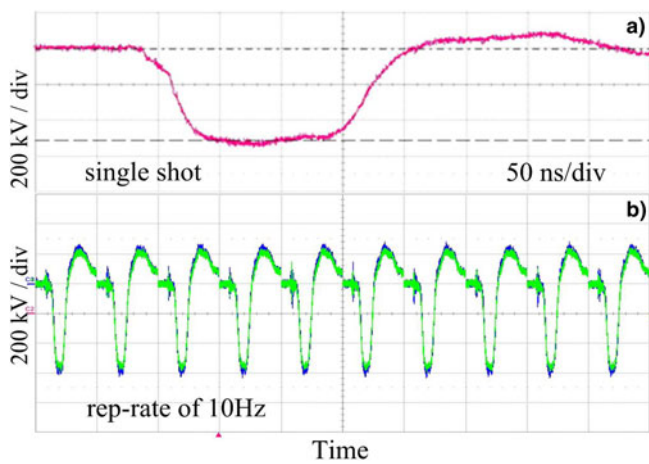


Fig. 27. Output waveforms of pulse generator based on Kapton-film dielectric line at (a) single shot and (b) repetition rate of 10 Hz.

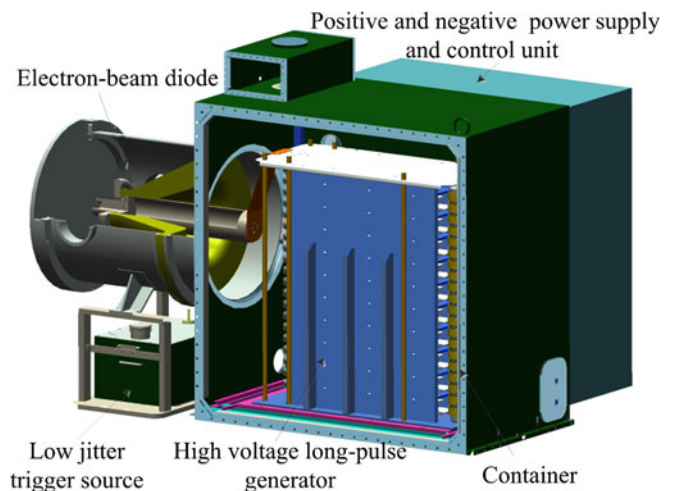



Fig. 28. Structural diagram of high pulse-energy repetitive PFN-Marx generator.

technology is inseparable from market demands, and the miniaturized pulsed power system needs to undergo a transition from laboratory device to industrial equipment. The development of miniaturized pulsed power sources with a high average power-to-volume ratio, high reliability, and long lifetime is one of the main directions for the future. To realize the market-oriented application of high-energy pulsed power sources, further researches are needed in the following aspects: (1) primary high-energy density storage technology, (2) pulse shaping and waveform control technology in compact structures, (3) high current switch with low jitter and long lifetime, (4) system thermal management technology.

Author ORCIDs.  Falun Song, 0000-0002-9666-6813.

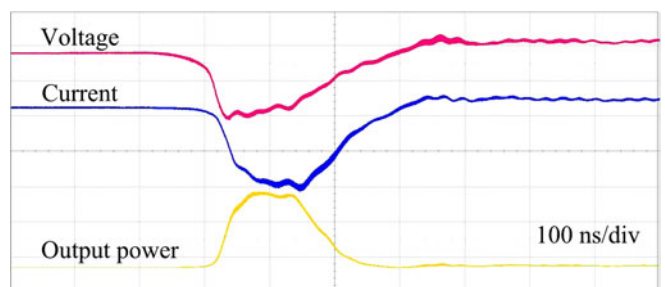


Fig. 29. The waveforms of 30 pulses on a plane diode.



Fig. 30. The photo of coaxial Marx generator.

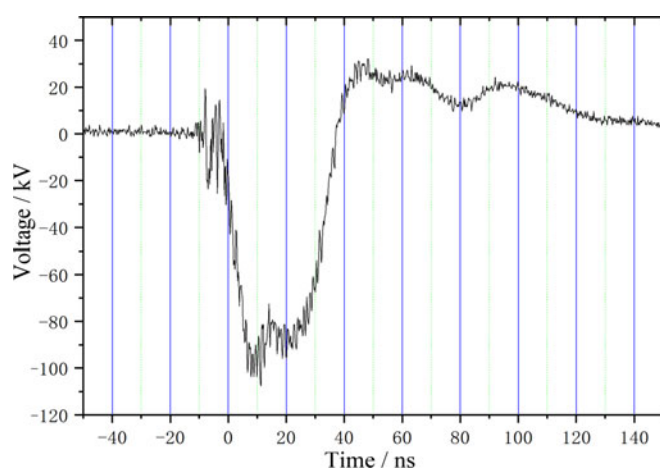


Fig. 31. A typical output waveform of coaxial Marx generator.

References

- Cao SY, Tan J, Fan ZK, Hu KS, Wu Y and Hou XQ (2006) Experimental study on helical Blumlein line. *High Power Laser and Particle Beams* **18**, 1046–1048.
- Deng JJ, Shi JS, Xie WP, Zhang LW, Feng SP, Li J, Wang M, Xia LS, Dai ZY, Li HT, Li Q, Wen L, Chen SF, Li X, Huang ZP, Lai QG, Zhang KZ, Xia MH, Guan YC, Song SY, Chen L, Ji C, Zhou LJ, He A, Zou WK, Huang XB, Zhou ST, Zhang ZH, Zhang SQ, Ren XB, Wei B, Tian Q, Yang AM, Li H, Xie M, Liu JF, Ma CG, Ma X, Wang W, Wang GJ, Yang LB, Gu YC, He Y, Li CG, Zhou YW, Zhang ZJ, Dai GS, Wang HC, Chen NA, Liu CJ, Sun CW, Xu Z, Meng FB and Ma HG (2015) Overview of pulsed power research at CAEP. *IEEE Transactions on Plasma Sciences* **43**, 2760–2765.
- Deng JJ, Xie WP, Feng SP, Wang M, Li HT, Song SY, Xia MH, Ji C, He A, Tian Q, Gu YC, Guan YC, Wei B, Huang XB, Ren XD, Dan JK, Li J, Zhou ST, Cai HC, Zhang SQ, Wang KL, Xu Q, Wang YJ, Zhang ZH, Wang GL, Guo S, He Y, Zhou YW, Zhang ZJ, Yang LB and Zou WK (2016) From concept to reality — a review to the primary test stand and its preliminary application in high energy density physics. *Matter and Radiation at Extreme* **1**, 48–58.
- Ding N, Zhang Y, Xiao DL, Wu JM, Dai ZH, Yin L, Gao ZM, Sun SK, Xue C, Ning C, Shu XJ and Wang JG (2016) Theoretical and numerical research of wire array Z-pinch and dynamic hohlraum at IAPCM. *Matter and Radiation at Extreme* **1**, 135–152.
- Gan YQ, Song FL, Zhuo TT, Qin F, Zhang Y, Gong HT and Jin X (2012) Design and experiment of portable Blumlein line. *High Power Laser and Particle Beams* **24**, 809–812.
- Gan YQ, Song FL, Zhuo TT, Zhang Y, Qin F, Gong HT and Jin X (2013) A compact repetitive Marx generator with fast risetime. *High Power Laser and Particle Beams* **25**(S0), 164–168.
- Gan YQ, Song FL, Lei F, Luo GY, Zhang BZ, Wang GP, Gong HT and Jin X (2018) Design and experimental research of high-power repetitive pulse charging power supply. *High Power Laser and Particle Beams* **30**, 065003.
- Gaudet JA, Barker RJ, Buchenauer CJ, Christodoulou C, Dickens J, Gundersen MA, Joshi RP, Krompholz HG, Kolb JF, Kuthi A, Laroussi M, Neuber A, Nunnally W, Schamiloglu E, Schoenbach KH, Tyo JS and Vidmar RJ (2004) Research issues in developing compact pulsed power for high peak power applications on mobile platforms. *Proceedings of the IEEE* **92**, 1144–1165.
- Kim AA, Kovalchuk BM, Kokshenev VA, Shishlov AV, Ratakhin NA, Oreshkin VI, Rostov VV, Koshelev VI and Losev VF (2016) Review of high-power pulsed systems at the Institute of High Current Electronics. *Matter and Radiation at Extreme* **1**, 201–206.
- Korovin SD, Rostov VV, Polevin SD, Pegel IV, Schamiloglu E, Fuks MI and Barker RJ (2004) Pulsed power-driven high-power microwave sources. *Proceedings of IEEE* **92**, 1082–1095.
- Lehr J and Ron P (2017) *Foundations of Pulsed Power Technology*. Hoboken, NJ: John Wiley & Sons, Inc.
- Li XW, Chang AB, Song FL, Qin F, Gan YQ, Gong HT and Jin X (2013) Design and experimental investigation of folded parallel-plate pulse forming line based on PCB. *High Power Laser and Particle Beams* **25**, 1826–1830.
- Li F, Song FL, Gan YQ, Jin X and Zhu MD (2017) Design and test on Marx trigger source with low output jitter. *Journal of Terahertz Science and Electronic Information Technology* **15**, 323–327.
- Li F, Song FL, Zhu MD, Jin X, Gan YQ and Gong HT (2018) A compact high-voltage pulse forming module with hundreds of nanoseconds quasi-squared output pulse. *Review of Scientific Instruments* **89**, 104706.
- Mesyats GA, Korovin SD, Gunin AV, Gubanov VP, Stepchenko AS, Grishin DM, Landl VF and Alekseenko PI (2003) Repetitively pulsed high-current accelerators with transformer charging of forming lines. *Laser and Particle Beams* **21**, 197–209.
- Mesyats GA, Korovin SD, Rostov VV, Shpak VG and Yalandin MI (2004) The RADAN series of compact pulsed power generators and their application. *Proceedings of IEEE* **92**, 1166–1179.
- Ouyang J, Liu YG, Liu JL, Wang MX and Feng JH (2008) Research on a folded Blumlein line using Kapton film as dielectrics. *Plasma Science and Technology* **10**, 231–234.
- Pan ZL, Yang JH and Cheng XB (2016) Research of the anti-resonance pulse forming network and its application in the Marx generator. *Laser and Particle Beams* **34**, 675–686.
- Qin F, Song FL, Gan YQ, Gong HT, Zhuo TT, Luo GY and Jin X (2012) Compact low-impedance Marx generator. *High Power Laser and Particle Beams* **24**, 907–911.
- Quintenz JP (2004) Overview of recent pulsed power advances at Sandia. *International Conference on High-Power Particle Beams*, Petersburg, Russia, pp. 27–32.

- Schamiloglu E, Schoenbach KH and Vidmar RJ** (2003) On the road to compact pulsed power: adventure in materials, electromagnetic modeling, and thermal management. *14th IEEE International Pulsed Power Conference*. Dallas, TX, USA, pp. 3–8.
- Smith I, Champney P, Hatch L, Nielsen K and Shope S** (1971) High current pulsed electron beam generator. *IEEE Transactions on Nuclear Science* **18**, 491–492.
- Song FL, Qin F, Zhuo TT, Gan YQ, Luo GY, Gong HT and Jin X** (2012) Design of layer-wound spiral strip dielectric film pulse forming line. *High Power Laser and Particle Beams* **24**, 659–612.
- Song FL, Gan YQ, Zhang Y, Qin F, Luo GY, Wang D, Chen DB, Wen J, Gong HT and Jin X** (2013). Compact low-impedance Marx generator for high power microwave applications. *High Power Laser and Particle Beams* **25**(S0), 177–181.
- Song FL, Jin X, Li F, Luo GY, Zhang BZ, Wang GP, Li CX, Su YB, Zhuo HY, Jin H, Gan YQ and Gong HT** (2017a) Progress on 20 GW compact repetitive Marx generator development. *High Power Laser and Particle Beams* **29**, 020101.
- Song FL, Li F, Qing F, Gan YQ, Luo GY, Gong HT and Jin X** (2017b) Design and experimental investigation of compact pulsed power source based on Kapton-film dielectric line. *High Power Laser and Particle Beams* **29**, 045004.
- Song FL, Li F, Zhang BZ, Gong HT, Gan YQ and Jin X** (2019) A compact low jitter high repetitive long-pulse relativistic electron beam source. *Nuclear Instruments and Methods in Physics Research Section A* **919**, 56–63.
- Xiang F, Tan J, Zhang YH, Wang GP, Luo M, Cao SY, Kang Q, Gong SG, Luo GY, Li CX, Jin H and Zhang BZ** (2010) Linear transformer driven long pulse high power generator with higher repetition rate. *Acta Physica Sinica* **59**, 4620–4625.
- Zhang YH, Chang AB, Xiang F, Song FL, Kang Q, Luo M, Li MJ and Gong SG** (2007) Repetition rate of intense current electron-beam diodes using 20GW Pulsed source. *Acta Physica Sinica* **56**, 5754–5757.
- Zhang JD, Ge XJ, Zhang J, He JT, Fan YW, Li ZQ, Jin ZX, Gao L, Ling JP and Qi ZM** (2016) Research progresses on Cherenkov and transit-time high-power microwave sources at NUDT. *Matter and Radiation at Extreme* **1**, 163–178.
- Zhang KY, Song FL, Zhang BZ, Zhang Q, Gan YQ, Gong HT and Jin X** (2018) Breakdown jitter characteristics of small field distortion gas switch. *High Power Laser and Particle Beams* **30**, 105003.